PLOS ONE

RESEARCH ARTICLE

Capsid Mutated Adeno-Associated Virus Delivered to the Anterior Chamber Results in Efficient Transduction of Trabecular Meshwork in Mouse and Rat

Barbara Bogner[1], Sanford L. Boye[2], Seok Hong Min[2], James J. Peterson[2], Qing Ruan[2], Zhonghong Zhang[1], Herbert A. Reitsamer[1], William W. Hauswirth[2], Shannon E. Boye[2]*

1 Department of Ophthalmology and Optometry, SALK/Paracelsus Medical University, Salzburg, Austria,
2 Department of Ophthalmology, University of Florida, Gainesville, United States of America

* Shannon.Boye@eye.ufl.edu

Citation: Bogner B, Boye SL, Min SH, Peterson JJ, Ruan Q, Zhang Z, et al. (2015) Capsid Mutated Adeno-Associated Virus Delivered to the Anterior Chamber Results in Efficient Transduction of Trabecular Meshwork in Mouse and Rat. PLoS ONE 10(6): e0128759. doi:10.1371/journal.pone.0128759

Academic Editor: Federico Mingozzi, University Pierre, FRANCE

Received: March 2, 2015

Accepted: April 30, 2015

Published: June 8, 2015

Data Availability Statement: All relevant data are within the paper.

Funding: This work was supported by: Doc-fFORTE-22966 (Austrian Academy of Sciences), PMU-FFF S-12/02/006-BOG, Lotte Schwarz Endowment for Experimental Ophthalmology and Glaucoma Research, Fuchs Endowment, Institutional Grant of the University Eye Clinic Salzburg, RO1 EY024280 (SEB), P30-EY021721 (WWH), and Research to Prevent Blindness.

Abstract

Background

Adeno associated virus (AAV) is well known for its ability to deliver transgenes to retina and to mediate improvements in animal models and patients with inherited retinal disease. Although the field is less advanced, there is growing interest in AAV's ability to target cells of the anterior segment. The purpose of our study was to fully articulate a reliable and reproducible method for injecting the anterior chamber (AC) of mice and rats and to investigate the transduction profiles of AAV2- and AAV8-based capsid mutants containing self-complementary (sc) genomes in the anterior segment of the eye.

Methodology/Principle Findings

AC injections were performed in C57BL/6 mice and Sprague Dawley rats. The cornea was punctured anterior of the iridocorneal angle. To seal the puncture site and to prevent reflux an air bubble was created in the AC. scAAVs expressing GFP were injected and transduction was evaluated by immunohistochemistry. Both parent serotype and capsid modifications affected expression. scAAV2- based vectors mediated efficient GFP-signal in the corneal endothelium, ciliary non-pigmented epithelium (NPE), iris and chamber angle including trabecular meshwork, with scAAV2(Y444F) and scAAV2(triple) being the most efficient.

Conclusions/Significance

This is the first study to semi quantitatively evaluate transduction of anterior segment tissues following injection of capsid-mutated AAV vectors. scAAV2- based vectors transduced corneal endothelium, ciliary NPE, iris and trabecular meshwork more effectively than scAAV8-based vectors. Mutagenesis of surface-exposed tyrosine residues greatly enhanced transduction efficiency of scAAV2 in these tissues. The number of Y-F mutations

Competing Interests: W.W.H. and the University of Florida have a financial interest in the use of AAV therapies and own equity in a company (AGTC, Inc.) that might, in the future, commercialize some aspects of this work.

was not directly proportional to transduction efficiency, however, suggesting that proteosomal avoidance alone may not be sufficient. These results are applicable to the development of targeted, gene-based strategies to investigate pathological processes of the anterior segment and may be applied toward the development of gene-based therapies for glaucoma and acquired or inherited corneal anomalies.

Introduction

Adeno associated virus (AAV)- mediated gene delivery has been used successfully to improve vision in animal models of inherited retinal disease and its safety/efficacy has also been proven in clinical trials [1–8]. In addition, AAV has been used to create animal models and investigate pathological mechanisms of ocular diseases e.g. in optic neuropathy [9] or age-related macular degeneration [10]. While transduction of the outer and inner retina is achievable via subretinal and intravitreal injection of AAV, respectively [11–13], these injection routes are not capable of, or at best, ill-suited for transducing tissues of the anterior segment. While the field is less advanced, there is a growing interest in targeting tissues like the trabecular meshwork (TM), which plays a role in the pathophysiology of glaucoma (reviewed in [14–17], and corneal layers, which can be affected by genetically determined non-inflammatory corneal dystrophies (reviewed in [18, 19]). Among others, targets of interest within the TM include pro-fibrotic and microfibril associated genes such transforming growth factor- beta (*TGFB*), connective tissue growth factor (*CTGF*), fibronectin (*FN*), bone morphogenic protein (*BMP*) and tissue transglutaminase (*tTG*) [15, 20–31]. Targets of interest in the cornea include carbohydrate sulfotransferase 6 (*CHST6*), keratin 3 (*KRT3*), keratin 12 (*KRT12*), a FYVE finger containing phosphoinositide kinase (*PIK5K3*), sodium bicarbonate transporter-like protein (*SLC4A11*), tumor associated calcium signal transducer 2 (*TACSTD2*), transforming growth factor, beta induced, 68 kDA (*TGFBI*) and UbiA prenyltransferase domain-containing protein 1 (*UBIAD1*) [18, 19]. Gene delivery to these tissues will require both a reliable injection technique and vectors that can efficiently transduce target cells *in vivo*. While other vectors have successfully been used to transduce these tissues [31–49], AAV is the preferred platform due to its inherent lack of immunogenicity, persistent transgene expression, ease of use (very rapid and facile cloning of vector constructs relative to other vector platforms) and clinical relevance in the eye.

Different AC (intracameral) injection methods have been described for delivering AAV in cynomolgus macaques, rats and mice [50–52]. Due to their small size and shallow anterior chambers, AC injections in mouse eyes are more challenging [52]. Gene delivery to outflow pathways via AC injection is preferred to intravitreal injection given the relatively small volume of the former. AC injection allows direct access to target tissues like TM and cornea with relatively little dilution effect (mouse AC volume is ~3 μl, mouse vitreous volume is ~10 μl) [53]. To date, all reports of AAV-mediated transduction of TM or cornea have focused on unmodified, first generation serotypes AAV1-AAV9 [49, 51, 54–58]. With the goal of targeting transgene expression to these tissues, we chose to focus on two 'parent' capsid serotypes, AAV2 and AAV8, as each has previously demonstrated utility for targeting TM and cornea, respectively [49, 51, 54, 57]. AAV2 transduces TM cells *in vitro*, organoculture [54], and TM in rat and non-human primate after intracameral injection [51]. The primary receptor for AAV2 is heparan sulfate proteoglycan (HSPG) [59, 60]. An abundance of HSPGs are found in the extracellular matrix and basement membranes of the TM, as is AAV2's co-receptor αVβ5 integrin [61]. HSPGs are also present in cornea [62]. Conversely, AAV8 does not bind HSPG [63].

However, studies show that this serotype efficiently transduces corneal stroma [27,29]. Thus, our selection was based on known AAV receptor biology and glycan footprints in target tissues.

The purpose of the current study was twofold. First, we aimed to investigate whether capsid mutated AAV vectors delivered via AC injection could efficiently transduce tissues of the anterior segment including TM and cornea. Our standard AAV vector vehicle (BSS supplemented with Tween 20) is low viscosity. We purposefully avoided using a high viscosity vehicle for injection because such 'gels' are composed of glycosaminoglycans (GAGs), which are the very substrates that AAV capsid's bind. Due to the low viscosity of injection solution and the small size/shallow anterior chamber in rodents, the propensity for vector reflux during injection was high. Our second aim, therefore, was to describe an anterior chamber injection method that was well tolerated and gave generally reproducible results in mice and rats with the goal of providing sufficient methodological detail for any labs interested in attempting similar experiments.

Methods

Experimental Animals

To establish the injection procedure and to investigate transduction profiles, male and female C57BL/6 mice and Sprague Dawley rats were used. All animal procedures were approved by the Institutional Animal Care and Use Committee on the Ethics of Animal Experiments of the University of Florida, Gainesville (IACUC Protocol # 201101103) and were carried out in strict accordance with the recommendations of the Association for Research in Vision and Ophthalmology (ARVO) Statement for the Use of Animals in Ophthalmic and Vision Research and the Guidelines for the Care and Use of Laboratory Animals of the National Institutes of Health. To ameliorate any pain or distress during ocular injections, rodents were anesthetized with intraperitoneal injection of ketamine/xylazine at a mixture of ketamine 80–120 mg/kg, xylazine 10–15 mg/kg. Rodents were humanely sacrificed by sedation first with ketamine/xylazine (as outlined above) followed by cervical dislocation in accordance with the University of Florida IACUC guidelines.

AAV-Vector Construction and Production

All scAAV serotypes and mutants contain the ubiquitous, truncated chimeric CMV-chicken β-actin (smCBA) promoter [64] driving the green fluorescent protein (GFP) reporter cDNA. AAV2 and AAV8 capsid mutants were generated by directed mutagenesis of highly conserved surface-exposed tyrosine and threonine residues with the QuickChange Multi Site-Directed Mutagenesis Kit (Agilent Technologies, CA 200514) as previously described[65–67]. Selected tyrosine and threonine residues were mutated to phenylalanine (Y–F) or valine (T–V), respectively. A summary of mutated residues and vector nomenclature are described in Table 1.

Table 1. AAV vectors and titers.

Construct	AAV Serotype	Titer (vg/mL)
sc-smCBA-hGFP	AAV2	~$2x10^{12}$
sc-smCBA-hGFP	AAV2(Y444F)	~$9x10^{11}$
sc-smCBA-hGFP	AAV2(Y444+500+730) (aka "AAV2(triple)")	~$3x10^{12}$
sc-smCBA-hGFP	AAV2(Y252+272+444+500+700+704+730F) (a.k.a. "AAV2(septuple)")	~$2x10^{12}$
sc-smCBA-hGFP	AAV8(Y733F)	~$2x10^{12}$

doi:10.1371/journal.pone.0128759.t001

scAAV vector preparations were performed by the 3-plasmid, co-transfection method according to methods described in detail previously [68–70]. Briefly, a calcium phosphate precipitation transfection was set up by mixing 500 μg: of vector plasmid "sc-trs-SB-smCBA-hGFP", 650 μg of plasmid coding for AAV2 'rep' and the variant specific 'cap' and 1550 μg of helper plasmid "pXX6" containing Adenovirus helper genes, respectively (**Table 1**). scAAV vector was titered for DNase-resistant vector genomes by quantitative real-time PCR against a known standard. Resulting titers are contained in Table 1.

Anterior Chamber Injections. Anterior Chamber Injections

AC injections were performed in C57BL/6 mice (injection volume 1 μl; age ~5 weeks; The Jackson Laboratory, Maine, USA) and Sprague Dawley rats (injection volume 2 μl; age ~12 weeks, Harlan Laboratories, USA). Mice (n = 35) and rats (n = 35) were anesthetized with a mixture of 100 mg/kg ketamine, 20 mg/kg xylazine and saline. Pupils were dilated with 1% atropine sulfate (Akorn, IL, USA) and 2.5% phenylephrine hydrochloride (Akorn, IL, USA). One drop of 0.5% proparacaine hydrochloride (Alcon, TX, USA) was applied to the cornea as a topical anesthetic. Animals were positioned slightly lateral and placed under a surgical microscope (Nikon SMZ800 fitted with Olympus Z4040Zoom camera). Hypromellose ophthalmic demulcent solution 2.5% (Gonak; Acorn, IL, USA) was applied onto the cornea to improve visibility when manipulating in the AC. Cornea was punctured with a 33-gauge needle (beveled 25° angle, 3-sharpening, with bevel up) just anterior of the iridocorneal angle. Care was taken not to disturb the iris or the lens (**Fig 1**). With a beveled 33-gauge needle we slowly injected approximately 200 nl air through the same puncture site at a rate of 30 nl/s. The needle was kept in position until the air bubble was fully formed and then slowly removed to facilitate gentle movement of the air bubble towards the puncture site (**Fig 1B**). When the bevel of the needle was close to the puncture site, it was pulled out quickly to keep the bubble at the puncture site.

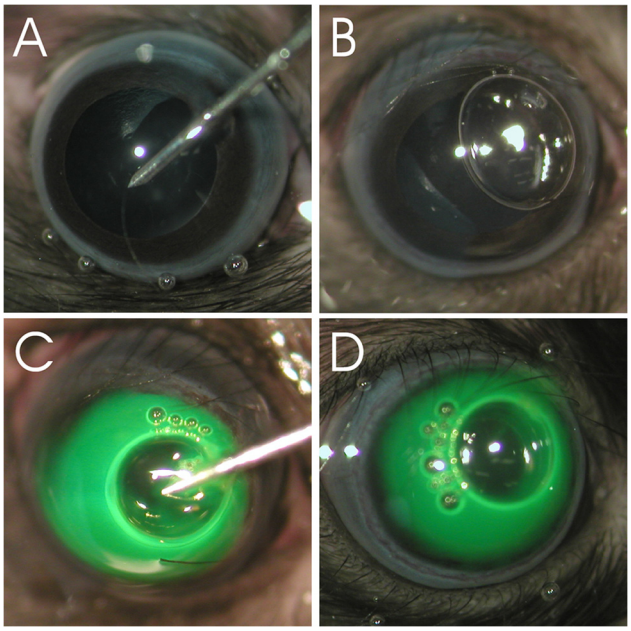

Fig 1. Injection procedure in mice. (A) The cornea is punctured closely anterior to the iridocorneal angle. (B) Before vector administration, an air bubble is created to seal the puncture site. (C-D) scAAV or vehicle dyed with fluorescein is injected. The air bubble seals the puncture site and reflux is minimized. The air bubble is absorbed within 24 hrs.

doi:10.1371/journal.pone.0128759.g001

Then, scAAV vectors expressing GFP under the constitutive small CMV-chicken β-actin (smCBA) promoter or vehicle control (BSS with 0.014% Tween-20) were injected via the same puncture site with the intraocular injection kit (WPI, Sarasota, USA) connected to a beveled, 33 gauge needle using a precision micropump (WPI, Sarasota, USA) (**Fig 1C**, **Table 2**). Fluorescein was added to each injection solution to visualize injections. To help the virus to diffuse away from the needle, it was infused slowly (30 nl/s in mice, 45 nl/s in rats). Before the needle was removed, it was held in position for 1 min. and care was taken to keep the air bubble at the puncture site in order to prevent reflux of vector/vehicle control. In some cases, repositioning of the air bubble was necessary to ensure a good seal. Neomycin, polymyxin B sulfate and dexamethasone ointment (Alcon, TX, USA) were applied to the eye after the procedure. Animals were placed on absorbent paper atop a 37°C heating plate for recovery and were then returned to their cages.

Immunohistochemistry

Eyes from scAAV-treated or mock-injected mice/rats were enucleated 4 weeks post-injection and fixed in 4% paraformaldehyde (PFA) for 1 to 2 hrs. Before the eyes were rinsed in 1xPBS (overnight) and soaked in 30% sucrose in 1xPBS (at least 12 hrs.) they were separated slightly anterior of the equator into the anterior and the posterior segment and the lens was carefully removed. Then, the divided eyes were immersed in OCT (Tissue Tek OCT 4583: Sakura Finetek USA, Inc., Torrance, CA), quick frozen in a bath of dry ice/ethanol and stored at -20°C until sectioning. Per eye, eight 10 micron cross sections in different planes were obtained by moving through tissue in a lateral to medial direction. For immunohistochemistry, all samples were prepared in parallel and processed identically. The sections from the anterior part of the eye were permeated and blocked with TBS containing 1% BSA, 0.1% Triton-X100 and species-matched normal serum for 1 hr. at room temperature (RT). To enhance the endogenous GFP-expression signal, sections were incubated with rabbit polyclonal GFP antibody [71] (1:1000, generously provided by Dr. Clay Smith, University of Florida) over night at 4°C. Alexa 488-conjugated secondary antibody (1:1000; Life Technologies, Germany) was applied for 1 hr. at RT. Nuclei were counterstained with 4',6-diamidino-2-phenylindole (DAPI) (1:2000; Merck, Austria). Between each incubation step and after DAPI application, washing steps of 3 x 5 min. were performed. The slides were mounted in TBS-Glycerin pH 8.6 and analyzed by confocal microsopy (LSM 710, Zeiss, Germany). In a subset of animals GFP and Thrombospondin-1 (TSP-1) double-labeling was performed to identify TM structures. TSP-1 is a matricellular protein (= extracellular protein modulating cell function and regulating cell surface and matrix

Table 2. Experimental groups of titer-matched scAAV-injected and mock-injected eyes.

Group	AAV Serotype	n
1	AAV2	5
2	AAV2(Y444F)	5
3	AAV2(triple)	5
4	AAV2(septuple)	5
5	AAV8(Y733F)	5
6	vehicle control	5
7	no injection	5

A sample size of 5 eyes per group was analyzed by immunohistochemistry for GFP-expression. The experimental protocol was performed in C57BL/6 mice and Sprague Dawley rats.

doi:10.1371/journal.pone.0128759.t002

interaction [72, 73]) that is produced and secreted by TM cells and is described to be present in the juxtacanalicular TM region [20, 74] and throughout the TM [75]. It was thus used as a marker to distinguish TM structures from others in the anterior chamber angle. Sections were incubated with mouse monoclonal TSP-1 antibody (clone A6.1 1:50; Thermo Fisher Scientific Inc., USA) and subsequently with an Alexa 555-conjugated secondary antibody.

Results

A Reliable Method for AC Injection in Rodent

A correctly positioned air bubble minimized reflux after AC injection of AAV contained within a low viscosity storage buffer (BSS +Tween 20) (**Fig 1**). The air bubble was absorbed within 24 hrs. and did not harm the ocular tissues. No signs of inflammation were observed after injection. Although care was taken to avoid any irritation of ocular tissues, we assume that the cornea of 1 mouse and 1 rat eye (in total 18 rats and 18 mice were injected; 3 animals of each species served as untreated control) may have been disturbed during the injection procedure, thus leading to inadvertent intrastromal delivery of AAV vectors and transduction of corneal stromal keratinocytes.

scAAV2-based Vectors Efficiently Transduce Tissues of the Anterior Segment

At four weeks post injection, eyes injected with scAAV2-based vectors exhibited GFP expression in the corneal endothelium, the ciliary non-pigmented epithelium (NPE), the iris and the chamber angle including the TM (**Fig 2**and **Fig 3**). Localization and semiquantitative evaluation of the GFP-signal in injected eyes are summarized in Table 3. For the semiquantitation, we used a grading system based on the presence of GFP-positive cells/structures in the anterior segment and the distribution of GFP-signal. Similar grading systems have previously been used to evaluate viral vector-mediated transduction of ocular tissues, including AAV [76, 77]. Four scores were defined: (1) no immunopositivity (-), (2) isolated positive cells/structures (-/+), (3) isolated to mosaic-like immunopositivity of cells/structures (+) and (4) mosaic-like to almost homogenous immunopositivtiy (++). The overall score was based on analysis of eight, 10 micron sections per eye by three independent examiners. Representative sections were chosen for illustration. The data show that scAAV2(Y444F) and scAAV2(triple) were highly efficient in transducing tissues of the anterior segment, whereas scAAV2 and scAAV2(septuple) showed only low efficiency. scAAV2(Y444F) and scAAV2(triple) had titers of ~9 x 10^{11} and ~3 x 10^{12}, respectively (Tables 1 and 3). It is possible that the slightly higher transduction efficiency observed with the triple vs. the single mutant resulted from the former being injected at a higher dose. In one out of five scAAV2(triple)- (**Fig 4A** and **Fig 4B**) and scAAV8(Y733F)- (**Fig 4C** and **Fig 4D**) injected eyes, GFP expression was detected in corneal stromal keratinocytes, a result likely owed to inadvertent intrastromal delivery. scAAV2(triple)-mediated GFP expression was more robust than that of scAAV8(Y733F). However, in general, GFP expression was absent from rodent eyes injected with scAAV8(Y733F). Depending on the scAAV variant used, the GFP-expression pattern ranged from isolated cells/structures to mosaic-like and homogenous (**Fig 2**and **Fig 3**). GFP was absent from both mock- injected (vehicle only) and uninjected eyes. Co-staining with TSP-1 in rat indicates that scAAV2(Y444F) and scAAV2(triple) transduced the TM structures (**Fig 5**). Both scAAV2(Y444F) and scAAV2(triple) transduced NPE of mice and rats very effectively. In contrast, scAAV2 and scAAV2(septuple) transduced only mouse NPE indicating that species differences may exist. No GFP-expression was present in the NPE of scAAV8(Y733F)- injected animals. Transduction of iris also appeared partly

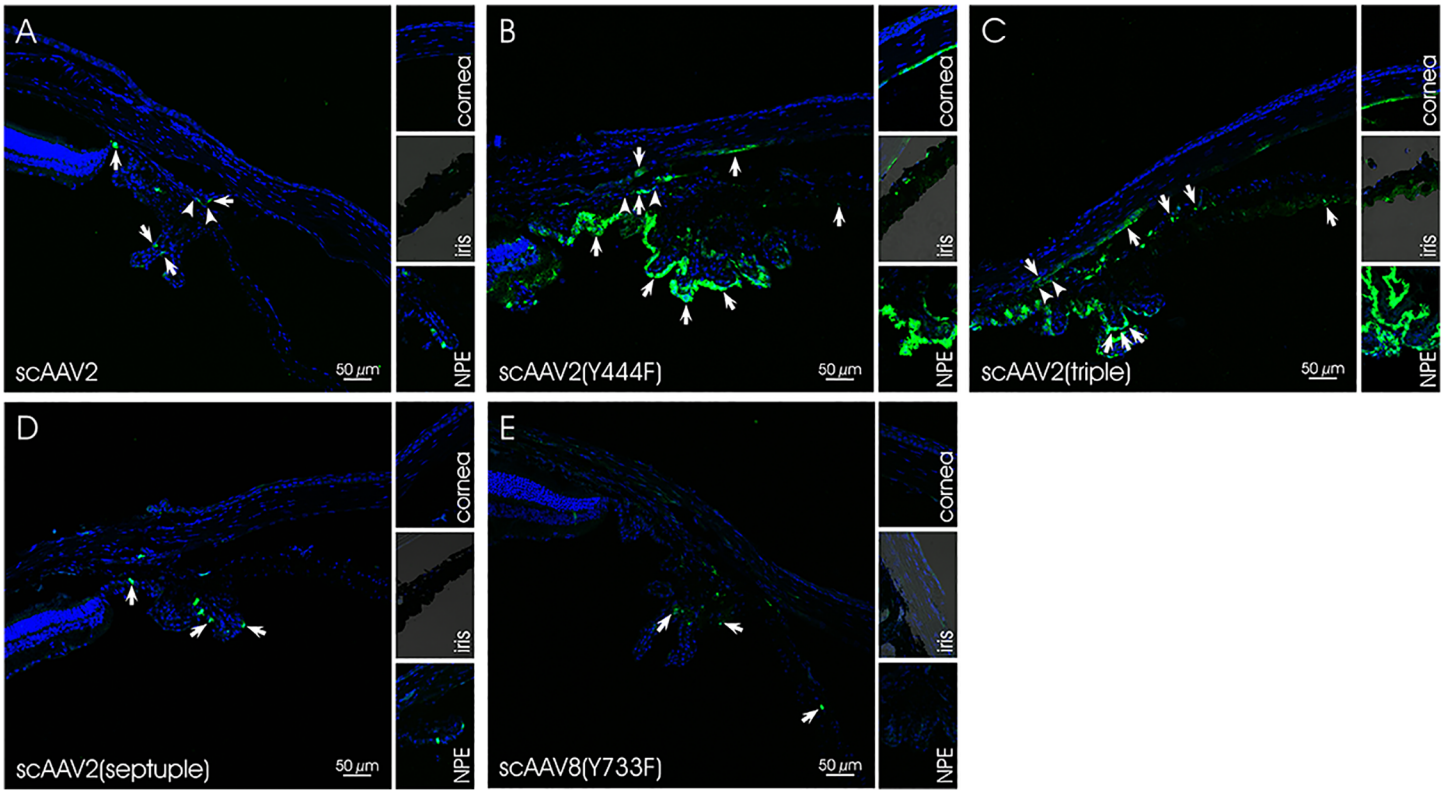

Fig 2. GFP expression in scAAV-injected mouse eyes. In A-D, representative sections of the region around the chamber angle are shown. The small inserts illustrate the cornea, the iris and the NPE. Nuclei are stained with DAPI. Arrows indicate GFP signals in the cornea, the iris, the chamber angle, the ciliary body and/or the NPE. Arrowheads mark the region of the TM.

doi:10.1371/journal.pone.0128759.g002

dependent on the species (Table 3). Corneal endothelium of mice and rats was effectively transduced by scAAV2(triple), whereas scAAV2(Y444F) only transduced corneal endothelium in mice efficiently.

Discussion

In this study, we established the transduction profiles of enhanced, capsid- mutated AAV vectors carrying self-complementary genomes following AC injection in mouse and rat. All previous reports of AAV-mediated transduction of AC tissues such as TM or corneal stroma have focused on unmodified, first generation serotypes AAV1-AAV9 [49, 51, 54–58]. However, the AAV vector toolkit is rapidly expanding and by combining knowledge of AAV capsid sequences with the structures available for these serotypes [78–83] (and unpublished data), it is now possible to delineate determinants of vector function (both intracellular and extracellular) and to rationally design vectors with desired biological properties [12, 84, 85]. For example, the three dimensional structure of AAV2 was used to identify capsid surface tyrosine, threonine, and serine residues, reported to promote ubiquitination and subsequent proteosomal degradation [67, 86]. Substitution of these residues significantly increased transduction efficiency and kinetics relative to unmodified virus in various tissues [65, 67, 87–89]. This approach was recently extended to the mutagenesis of lysine residues, which are directly ubiquitinated [86]. We have shown that, when subretinally delivered, Y-F mutants can restore function and preserve structure in multiple mouse models of retinal disease including the GC1KO and GCDKO mouse models of Leber congenital amaurosis-1 and the otherwise refractory *rd10* mouse

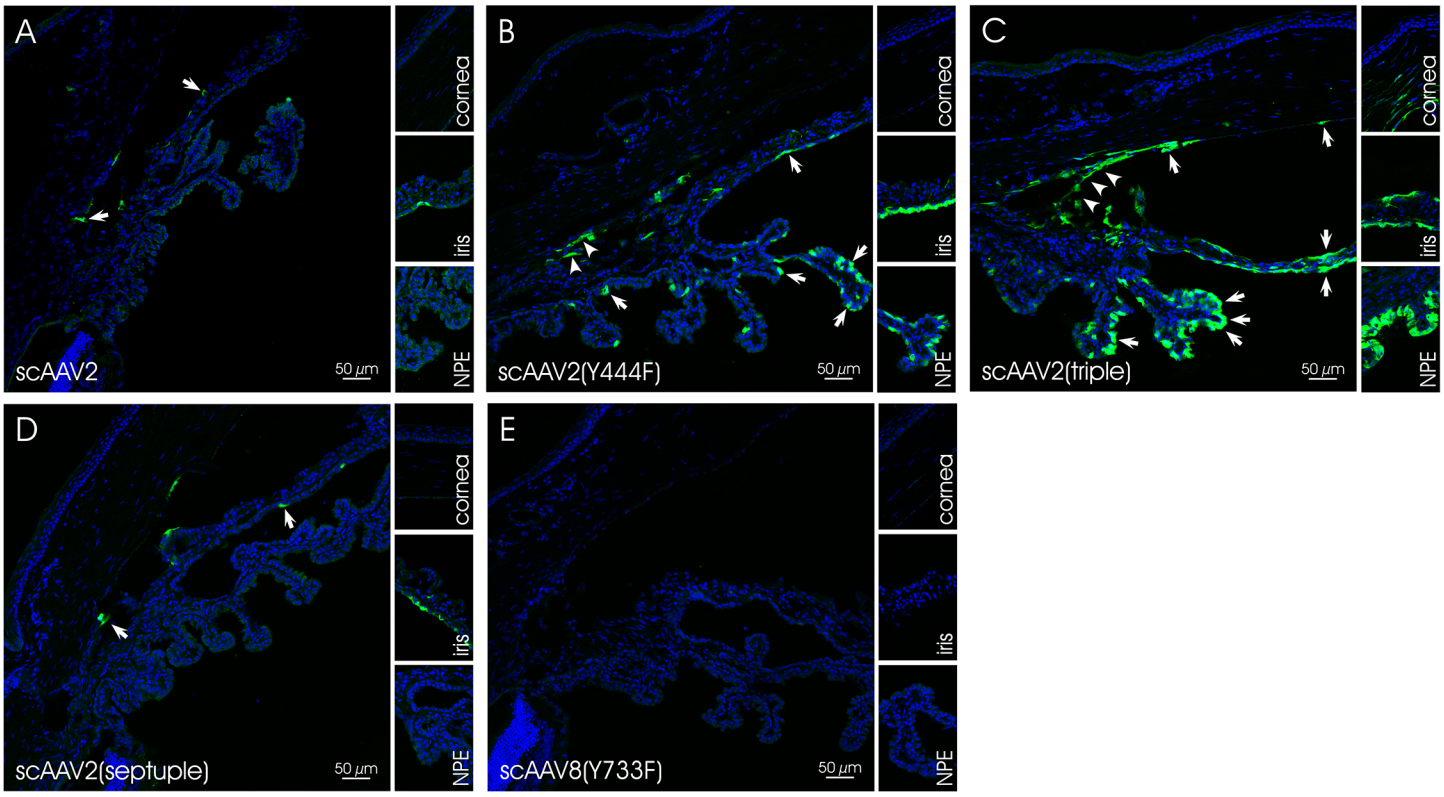

Fig 3. GFP expression in scAAV-injected rat eyes. In A-D, representative sections of the region around the chamber angle are shown. The small inserts illustrate the cornea, the iris and the NPE. Nuclei are stained with DAPI. Arrows indicate GFP signals in the cornea, the iris, the chamber angle and/or the NPE. Arrowheads mark the region of the TM.

doi:10.1371/journal.pone.0128759.g003

Table 3. Localization of the GFP signal in the anterior section of eyes injected with similar titers of scAAVs.

	Vector	C57BL/6 Mice (Injection Vol 1 μL)	Sprague Dawley Rats (Injection Vol 2 μL)
Group 1	scAAV2 WT~2x10^{12}	cornea—NPE + chamber angle + iris -	cornea—NPE—chamber angle + iris +
Group 2	scAAV2(Y444F) ~9x10^{11}	cornea + NPE ++ chamber angle ++ iris+	cornea—NPE ++ chamber angle ++ iris +
Group 3	scAAV2(triple) ~3x10^{12}	cornea ++*NPE ++ chamber angle ++ iris +	cornea ++*NPE ++ chamber angle ++ iris +
Group 4	scAAV(septuple) ~2x10^{12}	cornea—NPE-/+ chamber angle—iris -	cornea—NPE—chamber angle-/+ iris-/+
Group 5	scAAV8(Y733F) ~2x10^{12}	cornea -**NPE—chamber angle—iris-/+	cornea -**NPE—chamber angle—iris -

The transduction efficiency (grading:-,-/+, +, ++) is based on the intensity and distribution of the GFP signal in tissues of the anterior section. Unless otherwise noted (see asterisks) the term cornea represents GFP-expression in the corneal endothelium.

* One out of five showed GFP-positivity in the corneal stroma in addition to the corneal endothelium.

** One out of five showed GFP-positivity in the corneal stroma.

doi:10.1371/journal.pone.0128759.t003

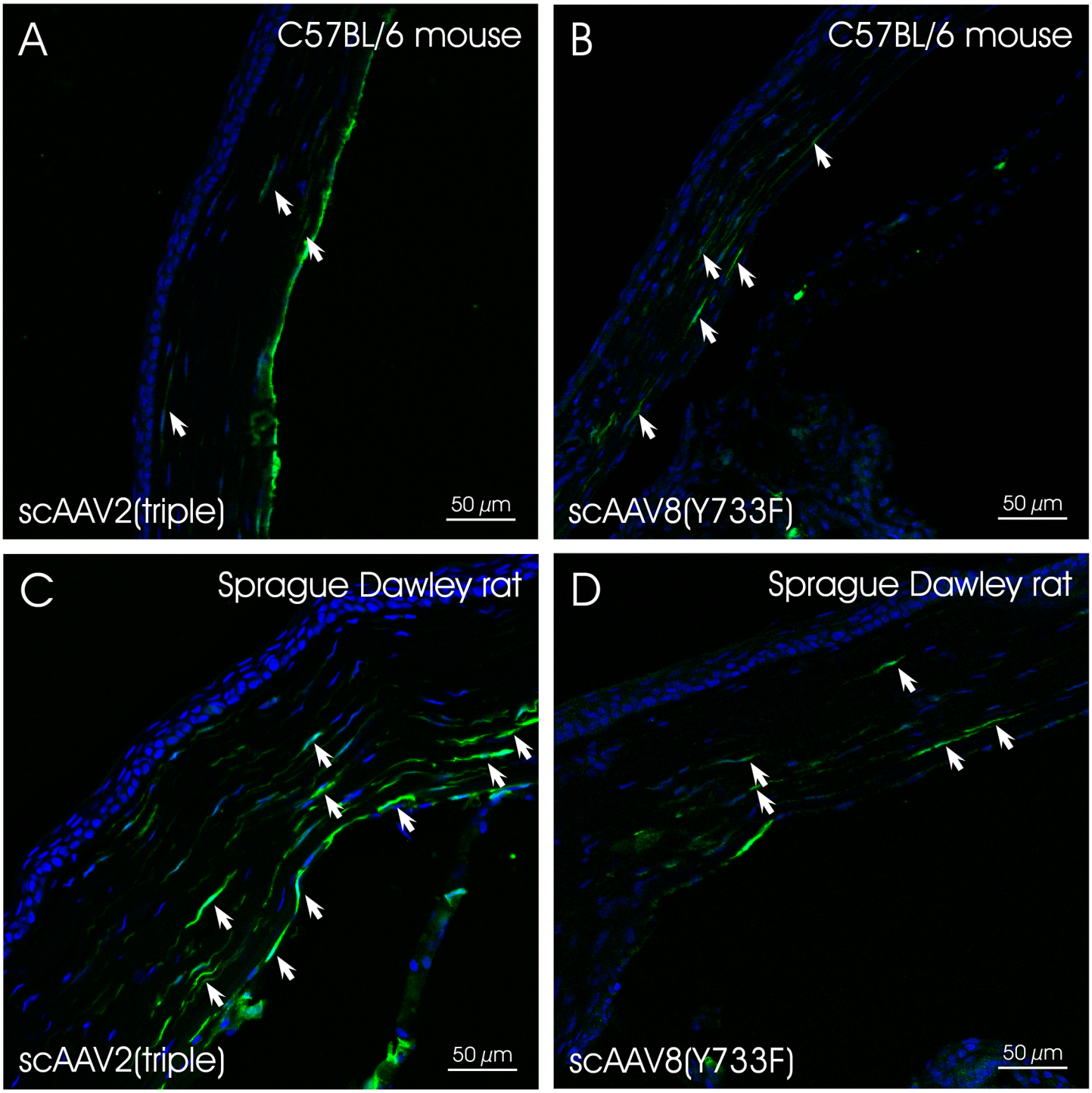

Fig 4. Corneas of scAAV2(triple)- and scAAV8(Y733F)- injected animals. GFP expression was detected in (A) scAAV(triple) and (B) scAAV8(Y733F)-injected mouse as well as in (C) scAAV2(triple)- and (D) scAAV8(Y733F)- injected rat corneas. Arrows indicate GFP- positive keratinocytes.

doi:10.1371/journal.pone.0128759.g004

model of autosomal recessive retinitis pigmentosa [90–92]. We chose to test similar AAV capsid variants for their ability to effectively transduce tissues in the anterior chamber such as TM and cornea. Because previous reports suggest that self-complimentary genomes are a

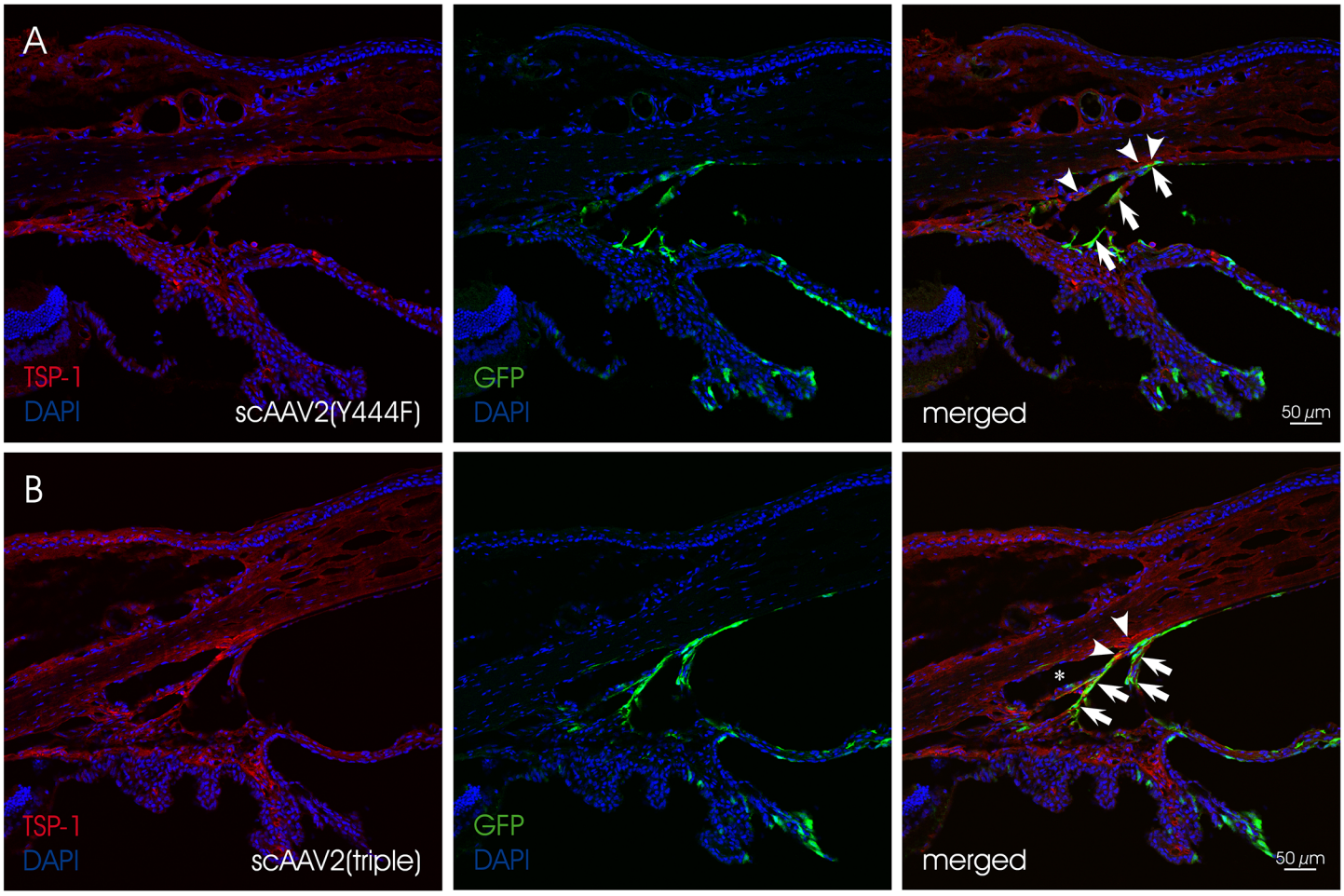

Fig 5. Co-staining of GFP (green, arrows) and TSP-1 (red, arrowheads) in chamber angle of injected rat eyes. (A) scAAV2(Y444F) and (B) scAAV2 (triple) mediate efficient transgene expression in the region of the trabecular meshwork. Nuclei are stained with DAPI. Asterisk indicates Schlemm's canal.

doi:10.1371/journal.pone.0128759.g005

requirement for TM transduction, we focused here only on scAAV vectors. Their ability to bypass rate-limiting second-strand DNA synthesis to obtain the transcriptionally active AAV genome results in earlier onset of transgene expression and thus a more rapid readout [93].

In previous studies, unmodified AAV2 and AAV8 vectors proved capable of targeting TM (intracameral injection) and cornea (intrastromal injection), respectively [49, 51, 54, 57]. This is likely owed to their respective receptor biology and the glycan footprint in target tissues. AAV2 binds HSPG, a proteoglycan abundant in TM and present in the cornea [59, 60]. AAV2's co-receptor, αVβ5 integrin is also found in the extracellular matrix of TM [61]. Conversely, AAV8 does not bind HSPG [63]. It is not surprising, therefore, that scAAV2(Y444F) and scAAV2(triple) vectors mediated relatively high levels of GFP expression in mouse and rat TM. Localization of AAV-mediated GFP signal in the TM was demonstrated by double-labeling with TSP-1 in rats. A previous study in rat [51] showed that AC-injected scAAV2 containing GFP driven by the human enhanced cytomegalovirus (CMV) promoter resulted in efficient transgene expression only after a period of 2.5 months. In contrast, our results show that scAAV2(Y444F)- and scAAV2(triple)- mediated GFP expression is robust by 4 weeks post-injection. As we did not evaluate transduction beyond 4 weeks we cannot determine conclusively whether scAAV2(Y-F) mutants simply lead to faster onset of expression. However, we note in

other ocular tissues (i.e. retinal ganglion cells, photoreceptors and retinal pigment epithelium), AAV2(Y-F) vectors consistently promote higher levels of transgene expression, for which early onset is the lead indicator [12, 13, 89, 94]. In our study we utilized the AAV8 capsid mutant (Y733F). While a direct comparison to unmodified AAV8 was not performed, existing data suggests that addition of the Y733F mutation does not result in changes of tropism [13]. We would therefor expect that un-modified scAAV8 vectors would lead to the same transduction pattern observed in this study.

An open question is whether efficient TM transduction relies on the use of self-complimentary genomes. Previously, Borras and colleagues found that co-infection of scAAV and recombinant Adenovirus with E1 and E3 deleted (rAdΔE1/E3) led to efficient transduction of TM [54]. They determined that single stranded AAV infection reduced expression of genes associated with DNA synthesis in the TM, which was reversed by the addition of rAdΔE1/E3. Use of scAAV vectors would overcome this rate limiting step and were hence tested. Interestingly, it has been shown that co-infection of AAV with empty Adenovirus capsid results in increased nuclear translocation of AAV [95]. Mechanistically, this is the same rationale for enhancement by the AAV(Y-F) variants [96]. It remains to be seen if these enhanced AAV2 capsid variants can overcome the need for utilization of a self-complementary gene cassette. This is of interest, as the canine model of spontaneous primary open angle glaucoma (POAG beagle), is associated with a mutation in the metalloproteinase ADAMTS10, which has a cDNA of 3312 bases, too large to be accommodated by scAAV vectors [97].

In addition to defining the transduction profile of scAAV2- and scAAV8- based capsid variants after AC injection, we also describe in detail a reliable AC injection technique for injecting low viscosity material in in both rat and mouse. This technique minimizes reflux, a common hurdle faced when delivering vector to this shallow chamber, and is reproducible, as evidenced by the repeatability of transduction by the efficient scAAV2 variants. Coupled with the diversity of genetically modified mouse strains, this approach will aid in elucidating biological processes of the anterior segment. Additionally, it impacts the development of gene-based therapies for the treatment of glaucoma and corneal disease/injury.

Acknowledgments

We acknowledge the outstanding, continuous support of experimental ophthalmology by Prof. Günther Grabner, MD and Chairman of the Dept. of Ophthalmology and Optometry at the Paracelsus Medical University/SALK Salzburg. Moreover, we thank Vince Chiodo and the RGTG staff for virus packaging and Renee Ryals for technical support.

Author Contributions

Conceived and designed the experiments: BB SLB SEB. Performed the experiments: BB SM JJP QR ZZ. Analyzed the data: BB SLB SEB. Contributed reagents/materials/analysis tools: HAR WWH. Wrote the paper: BB SLB SEB.

References

1. Boye SE, Boye SL, Lewin AS, Hauswirth WW. A comprehensive review of retinal gene therapy. MolTher. 2013; 21(3):509–19. doi: mt2012280 [pii];doi: 10.1038/mt.2012.280 PMID: 23358189
2. Bainbridge JW, Smith AJ, Barker SS, Robbie S, Henderson R, Balaggan K, et al. Effect of gene therapy on visual function in Leber's congenital amaurosis. NEnglJMed. 2008; 358(21):2231–9. doi: NEJMoa0802268 [pii];doi: 10.1056/NEJMoa0802268 PMID: 18441371
3. Cideciyan AV, Aleman TS, Boye SL, Schwartz SB, Kaushal S, Roman AJ, et al. Human gene therapy for RPE65 isomerase deficiency activates the retinoid cycle of vision but with slow rod kinetics.

ProcNatlAcadSciUSA. 2008; 105(39):15112–7. doi: 0807027105 [pii];doi: 10.1073/pnas.0807027105 PMID: 18809924

4. Hauswirth WW, Aleman TS, Kaushal S, Cideciyan AV, Schwartz SB, Wang L, et al. Treatment of leber congenital amaurosis due to RPE65 mutations by ocular subretinal injection of adeno-associated virus gene vector: short-term results of a phase I trial. HumGene Ther. 2008; 19(10):979–90. doi: 10.1089/hum.2008.107 PMID: 18774912
5. Maguire AM, Simonelli F, Pierce EA, Pugh EN Jr., Mingozzi F, Bennicelli J, et al. Safety and efficacy of gene transfer for Leber's congenital amaurosis. NEnglJMed. 2008; 358(21):2240–8. doi: NEJMoa0802315 [pii];doi: 10.1056/NEJMoa0802315 PMID: 18441370
6. Ashtari M, Cyckowski LL, Monroe JF, Marshall KA, Chung DC, Auricchio A, et al. The human visual cortex responds to gene therapy-mediated recovery of retinal function. JClinInvest. 2011; 121(6):2160–8. doi: 57377 [pii];doi: 10.1172/JCI57377 PMID: 21606598
7. Bennett J, Ashtari M, Wellman J, Marshall KA, Cyckowski LL, Chung DC, et al. AAV2 gene therapy readministration in three adults with congenital blindness. SciTranslMed. 2012; 4(120):120ra15. doi: 4/120/120ra15 [pii];doi: 10.1126/scitranslmed.3002865
8. Jacobson SG, Cideciyan AV, Ratnakaram R, Heon E, Schwartz SB, Roman AJ, et al. Gene therapy for leber congenital amaurosis caused by RPE65 mutations: safety and efficacy in 15 children and adults followed up to 3 years. ArchOphthalmol. 2012; 130(1):9–24. doi: archophthalmol.2011.298 [pii];doi: 10.1001/archophthalmol.2011.298 PMID: 21911650
9. Qi X, Sun L, Lewin AS, Hauswirth WW, Guy J. The mutant human ND4 subunit of complex I induces optic neuropathy in the mouse. Invest OphthalmolVisSci. 2007; 48(1):1–10.
10. Seo SJ, Krebs MP, Mao H, Jones K, Conners M, Lewin AS. Pathological consequences of long-term mitochondrial oxidative stress in the mouse retinal pigment epithelium. Experimental eye research. 2012; 101:60–71. Epub 2012/06/13. doi: 10.1016/j.exer.2012.05.013 PMID: 22687918; PubMed Central PMCID: PMC3419481.
11. Auricchio A, Kobinger G, Anand V, Hildinger M, O'Connor E, Maguire AM, et al. Exchange of surface proteins impacts on viral vector cellular specificity and transduction characteristics: the retina as a model. HumMolGenet. 2001; 10(26):3075–81. PMID: 11751689
12. Kay CN, Ryals RC, Aslanidi GV, Min SH, Ruan Q, Sun J, et al. Targeting photoreceptors via intravitreal delivery using novel, capsid-mutated AAV vectors. PLoSOne. 2013; 8(4):e62097. doi: 10.1371/journal.pone.0062097 PONE-D-13-07986 [pii]. PMID: 23637972
13. Petrs-Silva H, Dinculescu A, Li Q, Min SH, Chiodo V, Pang JJ, et al. High-efficiency transduction of the mouse retina by tyrosine-mutant AAV serotype vectors. MolTher. 2009; 17(3):463–71. doi: mt2008269 [pii];doi: 10.1038/mt.2008.269 PMID: 19066593
14. Rasmussen CA, Kaufman PL. The trabecular meshwork in normal eyes and in exfoliation glaucoma. Journal of glaucoma. 2014:S15-9. Epub 2014/10/03. doi: 10.1097/IJG.0000000000000106 PMID: 25275898.
15. Tektas OY, Lutjen-Drecoll E. Structural changes of the trabecular meshwork in different kinds of glaucoma. Experimental eye research. 2009; 88(4):769–75. Epub 2008/12/31. doi: 10.1016/j.exer.2008.11.025 PMID: 19114037.
16. Sacca SC, Pulliero A, Izzotti A. The dysfunction of the trabecular meshwork during glaucoma course. Journal of cellular physiology. 2014. Epub 2014/09/13. doi: 10.1002/jcp.24826 PMID: 25216121.
17. Borras T. Advances in glaucoma treatment and management: gene therapy. Invest Ophthalmol Vis Sci. 2012; 53(5):2506–10. Epub 2012/05/09. doi: 10.1167/iovs.12-9483o PMID: 22562852.
18. Klintworth GK. Corneal dystrophies. Orphanet journal of rare diseases. 2009; 4:7. Epub 2009/02/25. doi: 10.1186/1750-1172-4-7 PMID: 19236704; PubMed Central PMCID: PMC2695576.
19. Vemuganti GK, Rathi VM, Murthy SI. Histological landmarks in corneal dystrophy: pathology of corneal dystrophies. Developments in ophthalmology. 2011; 48:24–50. Epub 2011/05/05. doi: 10.1159/000324261 PMID: 21540630.
20. Tamm ER. The trabecular meshwork outflow pathways: structural and functional aspects. Experimental eye research. 2009; 88(4):648–55. Epub 2009/02/26. doi: 10.1016/j.exer.2009.02.007 PMID: 19239914.
21. Tripathi RC, Li J, Chan WF, Tripathi BJ. Aqueous humor in glaucomatous eyes contains an increased level of TGF-beta 2. Experimental eye research. 1994; 59(6):723–7. PMID: 7698265.
22. Tovar-Vidales T, Roque R, Clark AF, Wordinger RJ. Tissue transglutaminase expression and activity in normal and glaucomatous human trabecular meshwork cells and tissues. Invest Ophthalmol Vis Sci. 2008; 49(2):622–8. doi: 10.1167/iovs.07-0835 PMID: 18235007; PubMed Central PMCID: PMC2648869.

23. Prendes MA, Harris A, Wirostko BM, Gerber AL, Siesky B. The role of transforming growth factor beta in glaucoma and the therapeutic implications. The British journal of ophthalmology. 2013; 97(6):680–6. doi: 10.1136/bjophthalmol-2011-301132 PMID: 23322881.

24. Medina-Ortiz WE, Belmares R, Neubauer S, Wordinger RJ, Clark AF. Cellular fibronectin expression in human trabecular meshwork and induction by transforming growth factor-beta2. Invest Ophthalmol Vis Sci. 2013; 54(10):6779–88. doi: 10.1167/iovs.13-12298 PMID: 24030464; PubMed Central PMCID: PMC3799562.

25. Wordinger RJ, Fleenor DL, Hellberg PE, Pang IH, Tovar TO, Zode GS, et al. Effects of TGF-beta2, BMP-4, and gremlin in the trabecular meshwork: implications for glaucoma. Invest Ophthalmol Vis Sci. 2007; 48(3):1191–200. doi: 10.1167/iovs.06-0296 PMID: 17325163.

26. Gottanka J, Chan D, Eichhorn M, Lutjen-Drecoll E, Ethier CR. Effects of TGF-beta2 in perfused human eyes. Invest Ophthalmol Vis Sci. 2004; 45(1):153–8. PMID: 14691167.

27. Fleenor DL, Shepard AR, Hellberg PE, Jacobson N, Pang IH, Clark AF. TGFbeta2-induced changes in human trabecular meshwork: implications for intraocular pressure. Invest Ophthalmol Vis Sci. 2006; 47 (1):226–34. doi: 10.1167/iovs.05-1060 PMID: 16384967.

28. Welge-Lussen U, May CA, Lutjen-Drecoll E. Induction of tissue transglutaminase in the trabecular meshwork by TGF-beta1 and TGF-beta2. Invest Ophthalmol Vis Sci. 2000; 41(8):2229–38. PMID: 10892867.

29. Junglas B, Kuespert S, Seleem AA, Struller T, Ullmann S, Bosl M, et al. Connective tissue growth factor causes glaucoma by modifying the actin cytoskeleton of the trabecular meshwork. The American journal of pathology. 2012; 180(6):2386–403. doi: 10.1016/j.ajpath.2012.02.030 PMID: 22542845.

30. Junglas B, Yu AH, Welge-Lussen U, Tamm ER, Fuchshofer R. Connective tissue growth factor induces extracellular matrix deposition in human trabecular meshwork cells. Experimental eye research. 2009; 88(6):1065–75. doi: 10.1016/j.exer.2009.01.008 PMID: 19450452.

31. Shepard AR, Millar JC, Pang IH, Jacobson N, Wang WH, Clark AF. Adenoviral gene transfer of active human transforming growth factor-{beta}2 elevates intraocular pressure and reduces outflow facility in rodent eyes. Invest Ophthalmol Vis Sci. 2010; 51(4):2067–76. doi: 10.1167/iovs.09-4567 PMID: 19959644.

32. Vittitow JL, Garg R, Rowlette LL, Epstein DL, O'Brien ET, Borras T. Gene transfer of dominant-negative RhoA increases outflow facility in perfused human anterior segment cultures. Mol Vis. 2002; 8:32–44. PMID: 11889464.

33. Xue W, Wallin R, Olmsted-Davis EA, Borras T. Matrix GLA protein function in human trabecular meshwork cells: inhibition of BMP2-induced calcification process. Invest Ophthalmol Vis Sci. 2006; 47 (3):997–1007. doi: 10.1167/iovs.05-1106 PMID: 16505034; PubMed Central PMCID: PMC1592516.

34. Wang WH, McNatt LG, Pang IH, Millar JC, Hellberg PE, Hellberg MH, et al. Increased expression of the WNT antagonist sFRP-1 in glaucoma elevates intraocular pressure. The Journal of clinical investigation. 2008; 118(3):1056–64. doi: 10.1172/JCI33871 PMID: 18274669; PubMed Central PMCID: PMC2242621.

35. Spiga MG, Borras T. Development of a gene therapy virus with a glucocorticoid-inducible MMP1 for the treatment of steroid glaucoma. Invest Ophthalmol Vis Sci. 2010; 51(6):3029–41. doi: 10.1167/iovs.09-4918 PMID: 20089870; PubMed Central PMCID: PMC2891462.

36. Kumar S, Shah S, Tang HM, Smith M, Borras T, Danias J. Tissue plasminogen activator in trabecular meshwork attenuates steroid induced outflow resistance in mice. PloS one. 2013; 8(8):e72447. doi: 10.1371/journal.pone.0072447 PMID: 23977299; PubMed Central PMCID: PMC3747096.

37. Gerometta R, Spiga MG, Borras T, Candia OA. Treatment of sheep steroid-induced ocular hypertension with a glucocorticoid-inducible MMP1 gene therapy virus. Invest Ophthalmol Vis Sci. 2010; 51 (6):3042–8. doi: 10.1167/iovs.09-4920 PMID: 20089869; PubMed Central PMCID: PMC2891463.

38. Balaggan KS, Ali RR. Ocular gene delivery using lentiviral vectors. Gene Ther. 2012; 19(2):145–53. doi: 10.1038/gt.2011.153 PMID: 22052240.

39. Barraza RA, McLaren JW, Poeschla EM. Prostaglandin pathway gene therapy for sustained reduction of intraocular pressure. Mol Ther. 2010; 18(3):491–501. doi: 10.1038/mt.2009.278 PMID: 19953083; PubMed Central PMCID: PMC2839422.

40. Lipinski DM, Barnard AR, Charbel Issa P, Singh MS, De Silva SR, Trabalza A, et al. Vesicular stomatitis virus glycoprotein- and Venezuelan equine encephalitis virus-derived glycoprotein-pseudotyped lentivirus vectors differentially transduce corneal endothelium, trabecular meshwork, and human photoreceptors. Hum Gene Ther. 2014; 25(1):50–62. doi: 10.1089/hum.2013.009 PMID: 24125177.

41. Xiang Y, Li B, Wang JM, Li GG, Zhang H, Manyande A, et al. Gene transfer to human trabecular meshwork cells in vitro and ex vivo using HIV-based lentivirus. International journal of ophthalmology. 2014; 7(6):924–9. doi: 10.3980/j.issn.2222-3959.2014.06.02 PMID: 25540740; PubMed Central PMCID: PMC4270982.

42. Lee ES, Rasmussen CA, Filla MS, Slauson SR, Kolb AW, Peters DM, et al. Prospects for lentiviral vector mediated prostaglandin F synthase gene delivery in monkey eyes in vivo. Current eye research. 2014; 39(9):859–70. doi: 10.3109/02713683.2014.884593 PMID: 24559478; PubMed Central PMCID: PMC4134385.

43. Zhang Z, Dhaliwal AS, Tseng H, Kim JD, Schuman JS, Weinreb RN, et al. Outflow tract ablation using a conditionally cytotoxic feline immunodeficiency viral vector. Invest Ophthalmol Vis Sci. 2014; 55 (2):935–40. doi: 10.1167/iovs.13-12890 PMID: 24448264; PubMed Central PMCID: PMC3929079.

44. Parker DG, Kaufmann C, Brereton HM, Anson DS, Francis-Staite L, Jessup CF, et al. Lentivirus-mediated gene transfer to the rat, ovine and human cornea. Gene Ther. 2007; 14(9):760–7. doi: 10.1038/sj.gt.3302921 PMID: 17301843.

45. Mohan RR, Rodier JT, Sharma A. Corneal gene therapy: basic science and translational perspective. The ocular surface. 2013; 11(3):150–64. doi: 10.1016/j.jtos.2012.10.004 PMID: 23838017; PubMed Central PMCID: PMC3708266.

46. Mohan RR, Tovey JC, Sharma A, Tandon A. Gene therapy in the cornea: 2005—present. Prog Retin Eye Res. 2012; 31(1):43–64. doi: 10.1016/j.preteyeres.2011.09.001 PMID: 21967960; PubMed Central PMCID: PMC3242872.

47. Williams KA, Klebe S. Gene therapy for corneal dystrophies and disease, where are we? Current opinion in ophthalmology. 2012; 23(4):276–9. doi: 10.1097/ICU.0b013e3283541eb6 PMID: 22543480.

48. Kampik D, Ali RR, Larkin DF. Experimental gene transfer to the corneal endothelium. Experimental eye research. 2012; 95(1):54–9. doi: 10.1016/j.exer.2011.07.001 PMID: 21777585.

49. Hippert C, Ibanes S, Serratrice N, Court F, Malecaze F, Kremer EJ, et al. Corneal transduction by intrastromal injection of AAV vectors in vivo in the mouse and ex vivo in human explants. PloS one. 2012; 7 (4):e35318. doi: 10.1371/journal.pone.0035318 PMID: 22523585; PubMed Central PMCID: PMC3327666.

50. Buie LK, Karim MZ, Smith MH, Borras T. Development of a model of elevated intraocular pressure in rats by gene transfer of bone morphogenetic protein 2. Invest Ophthalmol Vis Sci. 2013; 54(8):5441–55. Epub 2013/07/04. doi: 10.1167/iovs.13-11651 PMID: 23821199; PubMed Central PMCID: PMC3743456.

51. Buie LK, Rasmussen CA, Porterfield EC, Ramgolam VS, Choi VW, Markovic-Plese S, et al. Self-complementary AAV virus (scAAV) safe and long-term gene transfer in the trabecular meshwork of living rats and monkeys. Invest Ophthalmol Vis Sci. 2010; 51(1):236–48. Epub 2009/08/18. doi: iovs.09-3847 [pii]doi: 10.1167/iovs.09-3847 PMID: 19684004; PubMed Central PMCID: PMC2869048.

52. Li G, Gonzalez P, Camras LJ, Navarro I, Qiu J, Challa P, et al. Optimizing gene transfer to conventional outflow cells in living mouse eyes. Experimental eye research. 2013; 109:8–16. doi: 10.1016/j.exer.2013.01.005 PMID: 23337742; PubMed Central PMCID: PMC3615119.

53. Remtulla S, Hallett PE. A schematic eye for the mouse, and comparisons with the rat. Vision research. 1985; 25(1):21–31. PMID: 3984214.

54. Borras T, Xue W, Choi VW, Bartlett JS, Li G, Samulski RJ, et al. Mechanisms of AAV transduction in glaucoma-associated human trabecular meshwork cells. The journal of gene medicine. 2006; 8 (5):589–602. Epub 2006/03/01. doi: 10.1002/jgm.886 PMID: 16506246.

55. Liu J, Saghizadeh M, Tuli SS, Kramerov AA, Lewin AS, Bloom DC, et al. Different tropism of adenoviruses and adeno-associated viruses to corneal cells: implications for corneal gene therapy. Mol Vis. 2008; 14:2087–96. PMID: 19023450; PubMed Central PMCID: PMC2584774.

56. Mohan RR, Tandon A, Sharma A, Cowden JW, Tovey JC. Significant inhibition of corneal scarring in vivo with tissue-selective, targeted AAV5 decorin gene therapy. Invest Ophthalmol Vis Sci. 2011; 52 (7):4833–41. Epub 2011/05/10. doi: 10.1167/iovs.11-7357 PMID: 21551414; PubMed Central PMCID: PMC3175954.

57. Sharma A, Tovey JC, Ghosh A, Mohan RR. AAV serotype influences gene transfer in corneal stroma in vivo. Experimental eye research. 2010; 91(3):440–8. doi: 10.1016/j.exer.2010.06.020 PMID: 20599959; PubMed Central PMCID: PMC2926174.

58. Mohan RR, Sharma A, Cebulko TC, Tandon A. Vector delivery technique affects gene transfer in the cornea in vivo. Mol Vis. 2010; 16:2494–501. PMID: 21139995; PubMed Central PMCID: PMC2997332.

59. Summerford C, Samulski RJ. Membrane-associated heparan sulfate proteoglycan is a receptor for adeno-associated virus type 2 virions. Journal of virology. 1998; 72(2):1438–45. Epub 1998/01/28. PMID: 9445046; PubMed Central PMCID: PMC124624.

60. Opie SR, Warrington KH Jr., Agbandje-McKenna M, Zolotukhin S, Muzyczka N. Identification of amino acid residues in the capsid proteins of adeno-associated virus type 2 that contribute to heparan sulfate proteoglycan binding. Journal of virology. 2003; 77(12):6995–7006. Epub 2003/05/28. PMID: 12768018; PubMed Central PMCID: PMC156206.

61. Acott TS, Kelley MJ. Extracellular matrix in the trabecular meshwork. Experimental eye research. 2008; 86(4):543–61. Epub 2008/03/04. doi: 10.1016/j.exer.2008.01.013 PMID: 18313051; PubMed Central PMCID: PMC2376254.

62. Schittny JC, Timpl R, Engel J. High resolution immunoelectron microscopic localization of functional domains of laminin, nidogen, and heparan sulfate proteoglycan in epithelial basement membrane of mouse cornea reveals different topological orientations. The Journal of cell biology. 1988; 107 (4):1599–610. PMID: 2459133; PubMed Central PMCID: PMC2115247.

63. Vandenberghe LH, Wang L, Somanathan S, Zhi Y, Figueredo J, Calcedo R, et al. Heparin binding directs activation of T cells against adeno-associated virus serotype 2 capsid. Nature medicine. 2006; 12 (8):967–71. doi: 10.1038/nm1445 PMID: 16845388.

64. Haire SE, Pang J, Boye SL, Sokal I, Craft CM, Palczewski K, et al. Light-driven cone arrestin translocation in cones of postnatal guanylate cyclase-1 knockout mouse retina treated with AAV-GC1. Invest OphthalmolVisSci. 2006; 47(9):3745–53. PMID: 16936082

65. Zhong L, Li B, Mah CS, Govindasamy L, Agbandje-McKenna M, Cooper M, et al. Next generation of adeno-associated virus 2 vectors: point mutations in tyrosines lead to high-efficiency transduction at lower doses. ProcNatlAcadSciUSA. 2008; 105(22):7827–32. doi: 0802866105 [pii];doi: 10.1073/pnas.0802866105 PMID: 18511559

66. Wang W, Malcolm BA. Two-stage PCR protocol allowing introduction of multiple mutations, deletions and insertions using QuikChange Site-Directed Mutagenesis. Biotechniques. 1999; 26(4):680–2. PMID: 10343905.

67. Aslanidi GV, Rivers AE, Ortiz L, Song L, Ling C, Govindasamy L, et al. Optimization of the capsid of recombinant adeno-associated virus 2 (AAV2) vectors: the final threshold? PloS one. 2013; 8(3):e59142. doi: 10.1371/journal.pone.0059142 PMID: 23527116; PubMed Central PMCID: PMC3602601.

68. Zolotukhin S, Byrne BJ, Mason E, Zolotukhin I, Potter M, Chesnut K, et al. Recombinant adeno-associated virus purification using novel methods improves infectious titer and yield. Gene Ther. 1999; 6 (6):973–85. PMID: 10455399

69. Zolotukhin S, Potter M, Zolotukhin I, Sakai Y, Loiler S, Fraites TJ Jr., et al. Production and purification of serotype 1, 2, and 5 recombinant adeno-associated viral vectors. Methods. 2002; 28(2):158–67. PMID: 12413414

70. Weitz AC, Behrend MR, Lee NS, Klein RL, Chiodo VA, Hauswirth WW, et al. Imaging the response of the retina to electrical stimulation with genetically encoded calcium indicators. Journal of neurophysiology. 2013; 109(7):1979–88. doi: 10.1152/jn.00852.2012 PMID: 23343890; PubMed Central PMCID: PMC3628009.

71. Peterson JJ, Tam BM, Moritz OL, Shelamer CL, Dugger DR, McDowell JH, et al. Arrestin migrates in photoreceptors in response to light: a study of arrestin localization using an arrestin-GFP fusion protein in transgenic frogs. Experimental eye research. 2003; 76(5):553–63. PMID: 12697419.

72. Bornstein P. Diversity of function is inherent in matricellular proteins: an appraisal of thrombospondin 1. The Journal of cell biology. 1995; 130(3):503–6. Epub 1995/08/01. PMID: 7542656; PubMed Central PMCID: PMC2120533.

73. Bornstein P. Thrombospondins as matricellular modulators of cell function. The Journal of clinical investigation. 2001; 107(8):929–34. Epub 2001/04/18. doi: 10.1172/JCI12749 PMID: 11306593; PubMed Central PMCID: PMC199563.

74. Flugel-Koch C, Ohlmann A, Fuchshofer R, Welge-Lussen U, Tamm ER. Thrombospondin-1 in the trabecular meshwork: localization in normal and glaucomatous eyes, and induction by TGF-beta1 and dexamethasone in vitro. Experimental eye research. 2004; 79(5):649–63. Epub 2004/10/27. doi: 10.1016/j.exer.2004.07.005 PMID: 15500824.

75. Hiscott P, Paraoan L, Choudhary A, Ordonez JL, Al-Khaier A, Armstrong DJ. Thrombospondin 1, thrombospondin 2 and the eye. Progress in retinal and eye research. 2006; 25(1):1–18. Epub 2005/07/06. doi: 10.1016/j.preteyeres.2005.05.001 PMID: 15996506.

76. Lebherz C, Maguire A, Tang W, Bennett J, Wilson JM. Novel AAV serotypes for improved ocular gene transfer. The journal of gene medicine. 2008; 10(4):375–82. doi: 10.1002/jgm.1126 PMID: 18278824; PubMed Central PMCID: PMC2842078.

77. Puppo A, Cesi G, Marrocco E, Piccolo P, Jacca S, Shayakhmetov DM, et al. Retinal transduction profiles by high-capacity viral vectors. Gene Ther. 2014; 21(10):855–65. doi: 10.1038/gt.2014.57 PMID: 24989814; PubMed Central PMCID: PMC4193889.

78. Asokan A, Schaffer DV, Samulski RJ. The AAV vector toolkit: poised at the clinical crossroads. Mol Ther. 2012; 20(4):699–708. doi: 10.1038/mt.2011.287 PMID: 22273577; PubMed Central PMCID: PMC3321598.

79. Xie Q, Bu W, Bhatia S, Hare J, Somasundaram T, Azzi A, et al. The atomic structure of adeno-associated virus (AAV-2), a vector for human gene therapy. Proc Natl Acad Sci U S A. 2002; 99(16):10405–10. doi: 10.1073/pnas.162250899 PMID: 12136130; PubMed Central PMCID: PMC124927.

80. Nam HJ, Lane MD, Padron E, Gurda B, McKenna R, Kohlbrenner E, et al. Structure of adeno-associated virus serotype 8, a gene therapy vector. Journal of virology. 2007; 81(22):12260–71. doi: 10.1128/JVI.01304-07 PMID: 17728238; PubMed Central PMCID: PMC2168965.

81. Padron E, Bowman V, Kaludov N, Govindasamy L, Levy H, Nick P, et al. Structure of adeno-associated virus type 4. JVirol. 2005; 79(8):5047–58. PMID: 15795290

82. DiMattia M, Govindasamy L, Levy HC, Gurda-Whitaker B, Kalina A, Kohlbrenner E, et al. Production, purification, crystallization and preliminary X-ray structural studies of adeno-associated virus serotype 5. Acta CrystallographSectFStructBiolCrystCommun. 2005; 61(Pt 10):917–21.

83. DiMattia MA, Nam HJ, Van Vliet K, Mitchell M, Bennett A, Gurda BL, et al. Structural insight into the unique properties of adeno-associated virus serotype 9. Journal of virology. 2012; 86(12):6947–58. doi: 10.1128/JVI.07232-11 PMID: 22496238; PubMed Central PMCID: PMC3393551.

84. Bowles DE, McPhee SW, Li C, Gray SJ, Samulski JJ, Camp AS, et al. Phase 1 gene therapy for Duchenne muscular dystrophy using a translational optimized AAV vector. Mol Ther. 2012; 20(2):443–55. doi: 10.1038/mt.2011.237 PMID: 22068425; PubMed Central PMCID: PMC3277234.

85. Klimczak RR, Koerber JT, Dalkara D, Flannery JG, Schaffer DV. A novel adeno-associated viral variant for efficient and selective intravitreal transduction of rat Muller cells. PLoSOne. 2009; 4(10):e7467. doi: 10.1371/journal.pone.0007467 PMID: 19826483

86. Gabriel N, Hareendran S, Sen D, Gadkari RA, Sudha G, Selot R, et al. Bioengineering of AAV2 capsid at specific serine, threonine, or lysine residues improves its transduction efficiency in vitro and in vivo. Human gene therapy methods. 2013; 24(2):80–93. doi: 10.1089/hgtb.2012.194 PMID: 23379478; PubMed Central PMCID: PMC3732126.

87. Aslanidi GV, Rivers AE, Ortiz L, Govindasamy L, Ling C, Jayandharan GR, et al. High-efficiency transduction of human monocyte-derived dendritic cells by capsid-modified recombinant AAV2 vectors. Vaccine. 2012; 30(26):3908–17. doi: 10.1016/j.vaccine.2012.03.079 PMID: 22497875; PubMed Central PMCID: PMC3356484.

88. Markusic DM, Herzog RW, Aslanidi GV, Hoffman BE, Li B, Li M, et al. High-efficiency transduction and correction of murine hemophilia B using AAV2 vectors devoid of multiple surface-exposed tyrosines. Mol Ther. 2010; 18(12):2048–56. doi: 10.1038/mt.2010.172 PMID: 20736929; PubMed Central PMCID: PMC2997584.

89. Petrs-Silva H, Dinculescu A, Li Q, Deng WT, Pang JJ, Min SH, et al. Novel properties of tyrosine-mutant AAV2 vectors in the mouse retina. MolTher. 2011; 19(2):293–301. doi: mt2010234 [pii];doi: 10.1038/mt.2010.234 PMID: 21045809

90. Boye SL, Conlon T, Erger K, Ryals R, Neeley A, Cossette T, et al. Long-term preservation of cone photoreceptors and restoration of cone function by gene therapy in the guanylate cyclase-1 knockout (GC1KO) mouse. Invest OphthalmolVisSci. 2011; 52(10):7098–108. doi: iovs.11-7867 [pii];doi: 10.1167/iovs.11-7867 PMID: 21778276

91. Pang JJ, Dai X, Boye SE, Barone I, Boye SL, Mao S, et al. Long-term retinal function and structure rescue using capsid mutant AAV8 vector in the rd10 mouse, a model of recessive retinitis pigmentosa. MolTher. 2011; 19(2):234–42. doi: mt2010273 [pii];doi: 10.1038/mt.2010.273 PMID: 21139570

92. Boye SL, Peshenko IV, Huang WC, Min SH, McDoom I, Kay CN, et al. AAV-mediated gene therapy in the guanylate cyclase (RetGC1/RetGC2) double knockout mouse model of Leber congenital amaurosis. HumGene Ther. 2013; 24(2):189–202. doi: 10.1089/hum.2012.193 PMID: 23210611

93. McCarty DM. Self-complementary AAV vectors; advances and applications. Mol Ther. 2008; 16 (10):1648–56. Epub 2008/08/07. doi: 10.1038/mt.2008.171 PMID: 18682697.

94. Koilkonda RD, Hauswirth WW, Guy J. Efficient expression of self-complementary AAV in ganglion cells of the ex vivo primate retina. Mol Vis. 2009; 15:2796–802. PMID: 20019878; PubMed Central PMCID: PMC2793898.

95. Xiao W, Warrington KH, Jr., Hearing P, Hughes J, Muzyczka N. Adenovirus-facilitated nuclear translocation of adeno-associated virus type 2. Journal of virology. 2002; 76(22):11505–17. PMID: 12388712; PubMed Central PMCID: PMC136768.

96. Zhong L, Li B, Mah CS, Govindasamy L, Agbandje-McKenna M, Cooper M, et al. Next generation of adeno-associated virus 2 vectors: point mutations in tyrosines lead to high-efficiency transduction at lower doses. Proc Natl Acad Sci U S A. 2008; 105(22):7827–32. Epub 2008/05/31. doi: 10.1073/pnas.0802866105 PMID: 18511559; PubMed Central PMCID: PMC2402387.

97. Kuchtey J, Olson LM, Rinkoski T, Mackay EO, Iverson TM, Gelatt KN, et al. Mapping of the disease locus and identification of ADAMTS10 as a candidate gene in a canine model of primary open angle glaucoma. PLoS genetics. 2011; 7(2):e1001306. Epub 2011/03/08. doi: 10.1371/journal.pgen.1001306 PMID: 21379321; PubMed Central PMCID: PMC3040645.